Engineered Science
DOI: https://dx.doi.org/10.30919/es8d777

Flexible Linear Low-density Polyethylene Laminated Aluminum and Nickel Foil Composite Tapes for Electromagnetic Interference Shielding

R. B. Jagadeesh Chandra,[1] B. Shivamurthy,[2,*] S. B. Bore Gowda[1] and M. Sathish Kumar[1]

Abstract

The increased usage of electronic systems creates electromagnetic interference (EMI). Many research studies are explored different types of materials for electromagnetic wave shielding. However, very limited work is carried out on electromagnetic wave shielding materials for flexible cables used in electronic equipment. In the current work, three types of flexible tapes, namely L-Al-L, L-Ni-L, and L-Ni-L-Al-L, were developed using foils of aluminum (Al) and Nickel (Ni) laminated with Linear low-density polyethylene (LLDPE) (L). The developed tapes were characterized for electromagnetic shielding. L-Al-L and L-Ni-L tape's average total shielding effectiveness was 34.8 dB with 59 % absorption and 37 dB with 65 % absorption, respectively. At the same time, the hybrid tape showed enhanced shielding effectiveness of 45 dB. However, compared to the other two tapes, the L-Al-L tape appeared to be a better material because it was low in cost, thin, more flexible, and easy to wrap around the cable during processing.

Keywords: Linear low-density polyethylene; Nickel foil; Aluminum foil; tapes for shielding; Flexible laminates; Absorption; Reflection.
Received: 11 April 2022; Revised: 20 September 2022; Accepted: 20 September 2022.
Article type: Research article

1. Introduction

The increased use of electronic devices has tremendously increased electromagnetic radiation (EMR) pollution and electromagnetic interference (EMI).[1] EMR hazards result in harmful biological effects on the human body. According to the experts, due to prolonged exposure to EMR, large number of people are suffering from cancer and other diseases. In addition, EMR affects data security, leakage and loss, and electronic system failure due to interference.[2] In particular, strong interference is created due to the high-frequency electromagnetic waves that are more harmful and lead to the disastrous failure of civil, military, electronic, and electrical devices.[3] Hence, the EMI shielding composite materials have evolved as a global concern. The carbonaceous fillers and metal foils that have good electrical and magnetic properties are used as shielding materials in the wide frequency range applications.

The cable that connects the critical electronic devices also needs EMI shielding in addition to insulation,[1] as shown in Fig. 1. An insulating jacket protects the wires against abrasion, moisture, and other outside environmental effects in an unshielded cable. However, it is not protected by electronic noise and EMI. Presently, various types of EMI shielding are used in cables, such as foils and braided shields. Shuangqiao Yang *et al.*[4] developed polyethylene/graphite nanoplatelet composites with 10–50 wt.% Graphene nanoplatelets (GNPs) having 10 µm & 100 µm lateral dimensions mixed with Linear low-density polyethylene (LLDPE) powder in a co-rotating twin-screw extruder. Further, the specimens were processed by injection and compression molding. The composites filled with GNP-10 and GNP-100 with 30 vol.% showed an increase in the volume electrical conductivity from 8.5 S/m to 29.9 S/m. The LLDPE/GNP-10 and LLDPE/GNP-100 with 50wt.% filler concentration exhibited EMI shielding performance of 33.8 and 37 dB, respectively, in the X- band frequency range. Noorunnisa Khanam *et al.*[5] investigated the effect of compounding conditions and filler concentration of the LLDPE reinforced with 1, 2, 4, 6, 8 and 10 wt.% GNP

[1] *Department of Electronics & Communication Engineering, Manipal Institute of Technology, Manipal Academy of Higher Education, Manipal-576104, India.*
[2] *Department of Mechanical & Industrial Engineering, Manipal Institute of Technology, Manipal Academy of Higher Education, Manipal-576104, India.*
**Email:* shiva.b@manipal.edu (B. Shivamurthy)

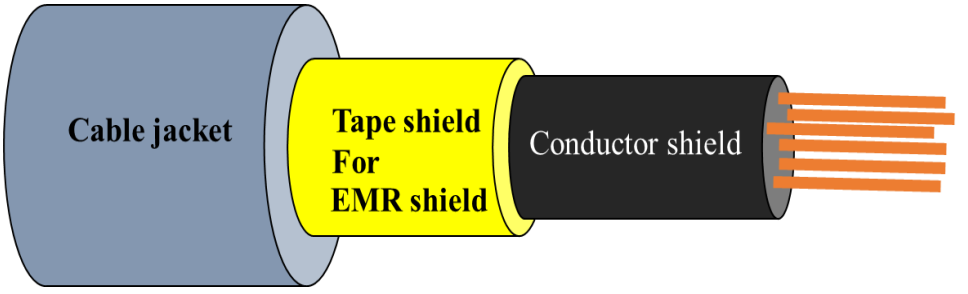

Fig. 1 Construction of cable suitable for EMR shielding.

composites on the mechanical, thermal, and electrical properties. Further, 4 wt.% GNPs in the LLDPE composites extruded with speeds of 50, 100, and 150 rpm showed an increase in the conductivity with an increase in the speed. They concluded 10wt.% GNP with 150 rpm had a conductivity of 8.94 $\times 10^{-5}$ S/m. Im *et al.*[6] developed GNP/Ni/PMMA multilayer nanocomposites by varying GNP/Ni fillers 20-40 wt.% insteps of 10 wt.% using solution blending. They found that the average conductivity of samples was increased with increase in the filler concentration from 29.18 to 412.62 S/m and the EMI shielding effectiveness of multilayer nanocomposites was 54-85 dB compared to monolayer 22-26 dB for the same thickness. They also developed GNP/Ni/Wax samples by a molecular-level mixing and ball-milling process with 0.7 mm thickness and showed shielding effectiveness of 48 and 20 dB, respectively.[7] Nimbalkar *et al.*[8] developed PC/GNPs nanocomposite by varying filler concentrations from 0 to 6 wt.% insteps of 0.5 wt.% using solution mixing followed by hot compaction. The 6 wt.% GNP nanocomposites exhibited shielding effectiveness of 35 dB at 8.2 GHz for 1 mm thickness, which showed an electrical conductivity of 0.413 S/m. Further, the same frequency shielding effectiveness increased to 47.2 dB at 2 mm thick. Sabira *et al.*[9] fabricated polyvinylidene fluoride/graphene nanocomposite films with a thickness of 20 µm that were prepared by solution casting with varying 2,5,10 and 15 wt.% filler loadings. They found that 15 wt.% graphene PVDF/Graphene nanocomposite films showed shielding effectiveness of 47 dB in the X-band frequency range. They observed that absorption was dominant. Joseph *et al.*[10] developed PMMA/Graphene and PVC/Graphene films and composites of 2 mm thickness that were prepared by solution casting followed by hot compression molding with filler loading concentrations of 1,5,10 and 20 wt.%. They found 20 wt% filler concentration with 2 mm thickness of PMMA/Graphene and PVC/Graphene composites showed EMI shielding effectiveness of 21 and 31dB, respectively, in the X-band frequency range.

Polymer composites are the combination of thermoset or thermoplastics with different conductive nanofillers. These polymer composites are used to develop hybrid polymer composite laminates with metal foils (i.e., silver, aluminum, and nickel). The polymer in the hybrid laminates results in good adhesion and protection from corrosion, improving bonding, flexibility, and EMI shielding properties.[11-13] Hence, in the current work, polymer-metal foil composite laminates are explored as suitable candidate for cable shielding.

Aluminum foil is a high electrical conductivity and low magnet permeability material. It is thin, flexible, low cost, and environmentally non-hazardous compared to lead. The aluminum foil has an electrical conductivity of 0.63 S/m and a magnet permeability of 1 H/m. Hence, it is considered as a shielding material in foil-type shielding.[14,15] However, aluminum foil shielding suffers due to low tensile strength and stiffness. According to EMI shielding theory, the EM wave reflects when it falls on an electrically conductive surface and is absorbed when it falls on a magnetic surface. Hence, in this work, we attempt to develop EMI shielding tapes by laminating aluminum foil with LLDPE. In addition, the LLDPE laminated nickel foil is also used to create hybrid tapes and investigate the reflection, absorption, and effective EMI shielding in the frequency range of the X-band.

2. Materials and Methods

2.1 Materials

The Extrusion-blowing method produced LLDPE film with average 75 µm thickness was purchased from M/s. Balaji poly pack, Shivamogga, Karnataka, India. The aluminum foil of 10-12 µm thickness and 100 µm thick nickel foil was from the local market in Mumbai.

2.2 Fabrication of multilayer composites

Three types of flexible laminated composite tapes such as (i) LLDPE-Aluminum foil- LLDPE (L-Al-L), (ii) LLDPE-Nickel foil-LLDPE (L-Ni-L), and (iii) LLDPE-Aluminum foil-LLDPE-Nickel foil- LLDPE (L-Al-L-Ni-L) were prepared by using LLDPE film, Aluminum-foil, and Nickel-foil. The foil and film were placed alternately one above the other and were hot-pressed at a temperature of about 150 °C in a 10-ton hydraulic press at 3 bar pressure[S_1]. Figs. 2 and 3 represent the arrangement of layers in flexible laminated composite and the thickness of the tapes prepared for EMI shielding.

2.3 Testing and characterization

The tensile properties of LLDPE film used for lamination were studied as per ASTM D 638.[16]), and a vector network analyzer with a waveguide was used to measure the EMI shielding effectiveness (SE_T) in the X band range (8-12) GHz.[17]

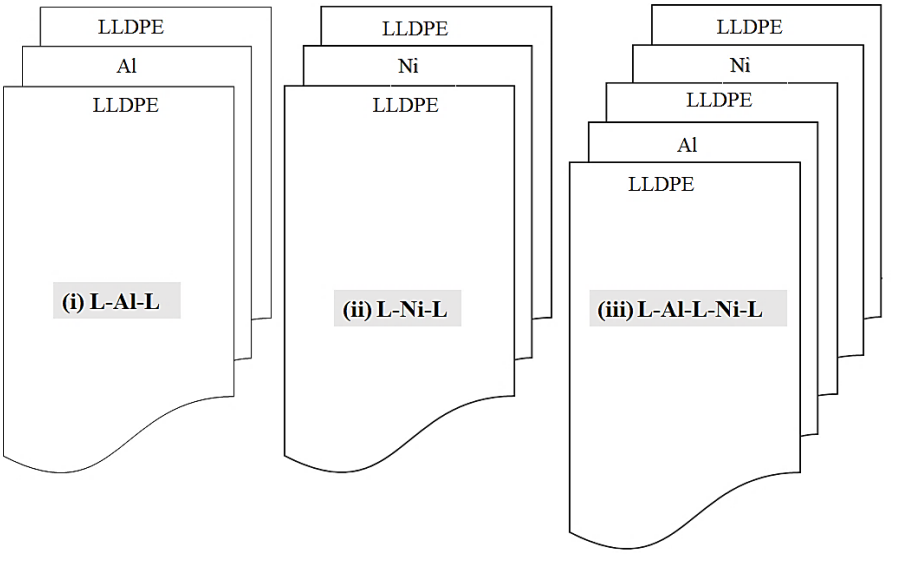

Fig. 2 Schematic arrangement of layers in flexible laminated composite tapes.

3. Results and discussions

3.1 Electrical conductivity

The electrical conductivity was measured as per ASTM D257.[18] The sample size of 5 × 5 mm was prepared with LLDPE5GNP, aluminum, and nickel films. The conductivity of the LLDPE5GNP, aluminum and nickel films are 2.72×10^{-7}, 2.95×10^{5}, and 1.46×10^{5} S/cm, respectively.

3.2 Skin depth

The skin depth (δ) is defined as the field strength of an RF signal on a material that drops to 1/e of its incident signal. The δ depends on the conductivity (σ), magnetic permeability (μ), operating frequency, and structure of the shielding material.[19] The high attenuation of RF energy dissipation is due to absorption, which implies excellent absorption properties. The skin depth is inversely proportional to absorption. The better EMI SE material should possess more significant absorption than reflection.[20]

The δ can be calculated as Equation (1):

$$\delta = 1/(\pi\sigma f \mu_r \mu_o)^{0.5} \quad (1)$$

If the thickness of the material and absorption are known, then δ can be calculated as Equation (2):

$$\delta = \frac{8.68 \times t}{SE_A} \quad (2)$$

The skin depth is calculated using Equation (2) and shown in Table 1.

Table 1. Skin depth of the prepared composites@8.2-10.4 GHz.

Sample	Thickness (mm)	Skin depth δ (mm)
L-Al-L	0.162	0.05 to 0.08
L-Ni-L	0.25	0.06 to 0.15
L-Al-L-Ni-L	0.337	0.8 to 0.12

The shielding effectiveness due to absorption can be calculated in terms of material thickness and skin depth as follows Equation (3):

$$SE_A = 8.7t\sqrt{\pi f \mu \sigma} \quad (3)$$

The absorption in the L-Al-L is 17.05 dB due to the conductivity of the composite. Similarly, L-Ni-L is 31.89 dB, and L-Ni-L-Al-L is 32.67 dB. This increase in the absorption is due to the synergetic effect of conductive and magnetic properties of the prepared composites at 0.06 mm skin depth at 10 GHz.

3.3 Tensile properties of LLDPE film

The tensile properties of LLDPE film were studied using a universal testing machine in the machined direction (MD) and the transverse direction (TD) with the strain rate of 0.02 S^{-1} as per ASTM 638D. The stress-strain values were plotted as shown in Fig. 4. The MD direction tensile strength at break is 26.4 MPa, which is higher than the TD direction tensile strength at break (18.6 MPa). The TD tensile strength is reduced; however, the elongation to break and stiffness are improved in the TD direction. The secant modulus in the MD direction is 0.65 GPa and 0.8 MPa in the TD direction. The averaged values of the three different film samples have been tabulated in Table 2. It is noticed that the elongation at break tends to respond opposite to the tensile strength, which is in line with the results published in the literature.[21] The increase in tensile strength in the MD direction is due to the orientation of molecules during extrusion. The GNPs are oriented in the machine direction during the drawing and blowing processes of film.[22] However, the mechanical properties of blown LLDPE film depend on other processing parameters such as die gap, throughput, blowing ratio, relaxation and crystallization effect. The higher MD direction tensile strength of LLDPE used for lamination is an advantage in the proposed EMI tapes for wrapping on the insulation of cables. In addition, the moderate TD direction strength witnesses the required tear strength in the TD direction.

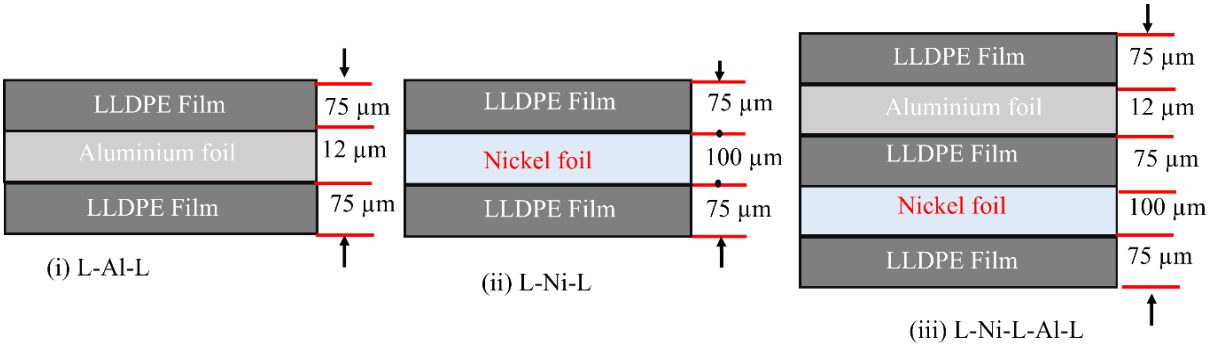

Fig. 3 The thickness of the prepared, flexible laminated composites (i) L-Al-L (ii) L-Ni-L (iii) L-Al-L-Ni-L.

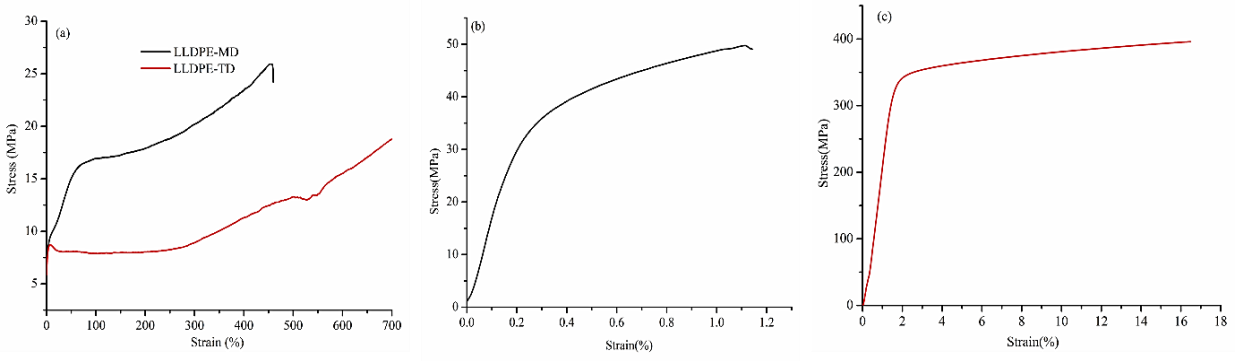

Fig. 4 Stress-Strain of (a) LLDPE film in MD and TD direction, (b) Aluminum foil, and (c) Nickel foil.

Table 2. Tensile properties of the raw material films.

Type of Film	Thickness (µm)	Tensile modulus (GPa)	Young's modulus (GPa)
LLDPE	75	Along MD=0.0264 Along TD=0.0186	NA
Ni	100	16.92	0.39
Al	12	12.95	0.049

3.4 Electromagnetic shielding effectiveness

The electromagnetic wave strikes the shielding material and experiences reflection, absorption, and multiple reflections. The reflection is due to an impedance mismatch in the shielding material and the incident electromagnetic wave.[23] However, the reflection losses also depend on the interaction of mobile charge carriers in the shielding material and radiation in the electromagnetic fields. The EMI shielding depends on the shielding material's properties and the EM wave's nature.[24] Good shielding material should have an absorption dominant as compared to reflection. The reflection (S_{11}) and transmission (S_{12}) scattering parameters were measured using S-parameters.[25]

$$R=|S_{11}|^2=|S_{22}|^2 \quad (4)$$

$$T=|S_{12}|^2=|S_{21}|^2 \quad (5)$$

The electromagnetic interference effectiveness of the material is the sum of absorption, reflection and multiple reflections.

$$SE_T=SE_A+SE_R+SE_{MR} \quad (6)$$

If absorption is above 10 dB, the multiple reflections are neglected.

The total EMI shielding according to:

$$SE_T=SE_A+SE_R \quad (7)$$

where A, R and T represents the absorption, reflection and transmission energy coefficients, respectively. However, SE_R, SE_A and SE_T represent the shielding effectiveness due to reflection, absorption and transmission, respectively.

$$SE_T\,(db) = 10\log_{10}\left(\frac{1}{S_{12}^2}\right) = 10\log_{10}\left(\frac{1}{S_{21}^2}\right) = \log_{10}\left(\frac{1}{T}\right) \quad (8)$$

$$SE_R\,(db) = 10\log_{10}\left(\frac{1}{1-S_{11}^2}\right) = 10\log_{10}\left(\frac{1}{1-R}\right) \quad (9)$$

$$SE_A\,(db) = 10\log_{10}\left(\frac{1-S_{11}^2}{S_{12}^2}\right) = 10\log_{10}\left(\frac{1-R}{T}\right) \quad (10)$$

The electromagnetic shielding due to absorption and reflection by the L-Al-L, L-Ni-L, and L-Al-L-Ni-L films was investigated using a 2-port N9911A vector network analyzer (Keysight Technologies, India) with a waveguide and sample holder as the arrangement shown in Fig. 5.

Three test samples from each composite tape and three samples of LLDPE film were accurately prepared to 22.86 mm ×10.16 mm and placed in the sample holder between the two waveguides. The reflection and transmission (S_{11} and S_{12}) scattering parameters were measured for X-band range frequencies. Before the measurement, the vector network analyzer calibration was performed. The SE_A, SE_R, and total electromagnetic interference shielding effectiveness (SE_T) can be evaluated from the S_{11}/S_{22} and S_{12}/S_{21} parameters using Equations (8), (9), and (10). The absorption, reflection, and total shielding effectiveness for all three types of tapes and LLDPE film in the X-band is shown in Figs. 6(a), (b), (c) and (d).

Figures 6(a) and 6(b) represent the attenuation of EM waves due to reflection (SE_R) and absorption mechanism (SE_A)

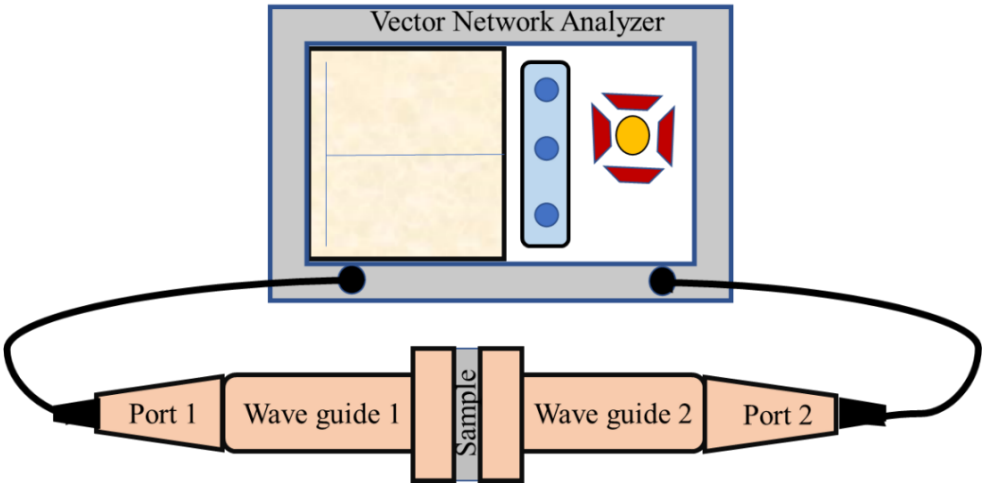

Fig. 5 Network analyzer experimental setup to measure S parameter.

and total shielding effectiveness (SE_T) in the X-band frequency range of L-Al-L and L-Ni-L tapes, respectively. In both types of tapes, the attenuation due to absorption and reflection is frequency-dependent. As observed from the slope of SE_A and SE_R curve from Figs. 6(a) and 6(b), in both types of tapes, the attenuation due to absorption increases with increasing frequency, but the attenuation by reflection increases with increasing frequency in the case of L-Al-L tape and reverse trend observed in case of L-Ni-L tape.

The magnetic radiation at higher frequency has lower wavelength and it is reflected by Al due to its electrical conductivity that is higher than Ni. The EMI shielding

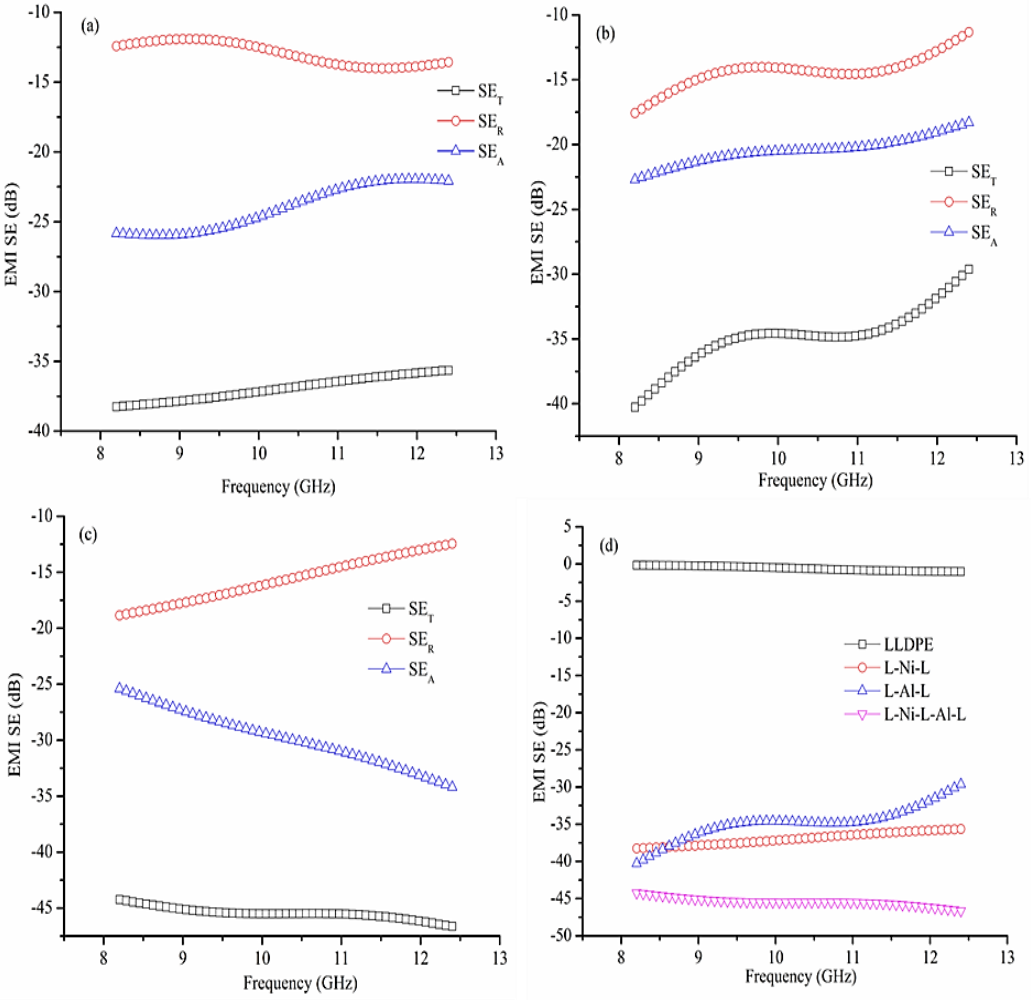

Fig. 6 Electromagnetic shielding effectiveness of LLDPE laminated Aluminum and Nickel foil composite tapes and LLDPE film in X-band; (a) SE_R, SE_A & SE_T of L-Al-L tape, (b) SE_R, SE_A & SE_T of L-Ni-L tape, (c) SE_R, SE_A & SE_T of L-Al-L-Ni-L tape and (d) SE_T of LLDPE film, L-Al-L, L-Ni-L & L-Al-L-Ni-L tapes.

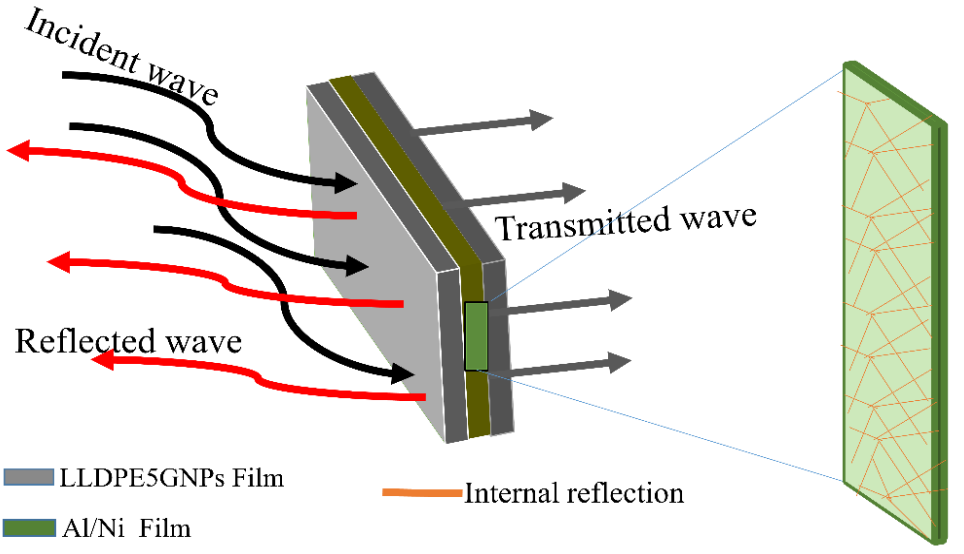

Fig. 7 Schematic EMI shielding mechanism for the LLDPE/Al composite.

mechanism in the prepared composites is shown in Fig. 7. The magnetic property of the Ni foil and its lower conductivity compared to Al foil synergistically influence on absorption mechanism of L-Ni-L tape. The total shielding effectiveness slightly decreases with increasing frequency in both types of tapes.

Similarly, Fig. 6(c) represents the attenuation of EM waves due to reflection (SE_R) and absorption mechanism (SE_A) and total shielding effectiveness (SE_T) in the X-band frequency range of L-Al-L-Ni-L hybrid tape. The observed attenuation due to absorption increases with increasing frequency, and a reverse trend is noticed in the reflection mechanism like L-Ni-L tape. However, the increase in the absorption as an increase in the frequency is comparatively more in L-Al-L-Ni-L tape than in L-Ni-L tape. It is found to have a higher slope of the SE_A curve in Fig. 6(c) compared to the SE_A curve in Fig. 6(b). This is due to the synergetic contribution of the high electrical conductivity of Aluminum foil and the high magnetic permeability of Nickel foil in the hybrid tape. The hybrid tape shows a shielding effectiveness of 45 dB, which is higher than that of L-Al-L and L-Ni-L tapes. However, the average shielding by absorption remains the same at around 65.5 % (refer to Figs. 6(a) and 6(b)). Although to the best of our knowledge, there hardly exists in the literature on the exact EMI shielding composite of the present work, a brief comparison of a similar line of works has been carried out. The comparison is given in Table 3. It is noted that the sample thickness in the current work is in the order of a few microns compared to the millimeter scale of the other works. Hence, the achieved EMI shielding appears to be appreciated.

Figures 8(a) and (b) show the average shielding percentage due to absorption and reflection and the average shielding effectiveness of the tapes, respectively. The average shielding effectiveness of L-Al-L and L-Ni-L tape is 34.8 dB with 59 % absorption and 37 dB with 65% absorption, respectively. The results found that the L-Ni-L tape shows slightly higher

Table 3. EMISE results of various similar works in the literature.

Matrix	Filler	Filler concentration	Sample thickness	EMISE (dB)	Frequency (GHz)	Reference
PMMA	GNP/Ni	20 ,30& 40 wt.%	0.83 mm each layer (3 layers)	61	8-12	[6]
Wax	GNP/Ni	30wt.%	0.7 mm	40	8-12	[7]
LLDPE	GNP10	50 wt.%	2.5 mm	33.8	8-12	[4]
	GNP100			37		
PC	GNP	0-6 wt.% in steps of 0.5 wt.%	0.5 mm	31.7	8-12	[8]
			2 mm	47.2		
PVDF	Graphene	15wt.%	20 μm	47	8-12	[9]
PMMA	Graphene	20 wt.%	2 mm	21		[10]
PVC	Graphene		2 mm	31		
LLDPE+5GNPs	Al	-	162 μm	34.8		Present work
	Ni		250 μm	37	8-12	
	Al-Ni		337 μm	45		

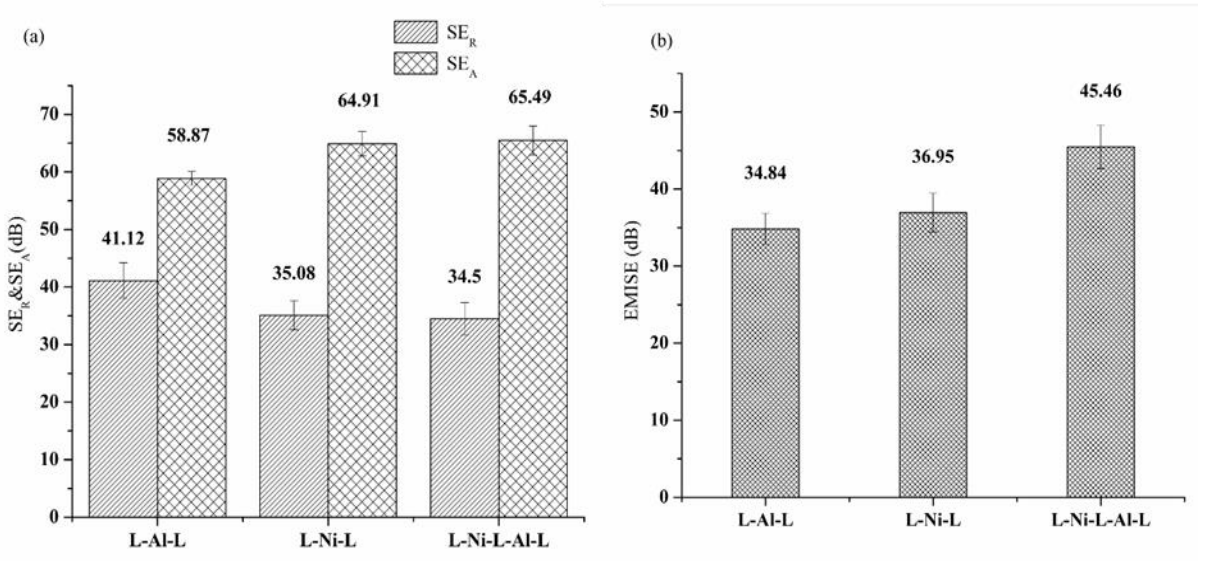

Fig. 8 (a) Average percentage of shielding due to absorption and reflection (b) Average total shielding effectiveness of the L-Al-L, L-Ni-L, and L-Ni-L-Al-L tapes.

absorption due to the high magnetic permeability of nickel; due to better electrical conductivity, the L-Al-L tape shows higher reflection. However, the L-Al-L tape is low-cost, thin, flexible, and easy to wrap around the cable while processing.

From Table 4, it is evident that the present work has better absorption per unit thickness compared to published works. However, L-Al-Ni is a better candidate for cable shielding application due to its mechanical strength, flexibility, and low cost.

Table 4. Comparison of the recently reported EMI shielding similar works in the X-band.

Samples	Thickness (d) mm	SE (dB)	SE_A dB	SE_A/d dB/mm	Reference
NPF	0.489	93.8	72.2	147.64	[19]
Ni chains/a-PSAs	0.18	39.97	25.75	143.05	[26]
1.5-DBSA-BF	0.4	37.72	30	75	[27]
BF/PANI	0.4	28.8	21.5	53.75	[28]
NaCF/PANI	0.4	48.83	40.47	101.17	[29]
L-Al-L	0.162	35	21	129.62	Present work
L-Ni-L	0.250	37	26	104	
L-Ni-L-Al-L	0.337	45	28	83.08	

4. Conclusion

Three types of EM wave shielding tapes are prepared using Aluminum, and Nickel foil laminated with LLDPE and found that the average total shielding effectiveness of L-Al-L-Ni-L is 45 dB, L-Ni-L is 37 dB, and L-Al-L is 35 dB in the X-band frequency range. All the tapes have shown that absorption is higher than reflection and are suitable to use in the X-band frequency range. However, the L-Al-L tape is attractive due to its low cost, thin, more flexible, and easier to wrap around the cable while processing.

Conflict of Interest

The authors declare no conflict of interest.

Supporting Information

Not applicable.

References

[1] M. Bayat, H. Yang, F. K. Ko, D. Michelson, A. Mei, Electromagnetic interference shielding effectiveness of hybrid multifunctional Fe_3O_4/carbon nanofiber composite, *Polymer*, 2014, **55**, 936-943, doi: 10.1016/j.polymer.2013.12.042.

[2] J. Zhang and Z. Yang, Electromagnetic Field Analysis and Shielding Method of Underground Variable Frequency Power Cable, *Advances in Civil Engineering*, 2022, **2022**, 3271806, doi: 10.1155/2022/3271806.

[3] A.G. Shcherbinin and R.P. Lukoyanov, Numerical Studies of the Electric Field of a Power Cable with Sector Strands and Impregnated Paper–Plastic Insulation for a Voltage of 20 kV, *Russian Electrical Engineering*, 2020, **91**, 698-702 doi: 10.3103/s1068371220110115.

[4] S. Yang, Z. Jin, C. Song, Z. Pu, B. Wen, The fabrication of polyethylene/graphite nanoplatelets composites for thermal management and electromagnetic interference shielding application, *Journal of Materials Science*, 2022, **57**, 1084-1097, doi: 10.1007/s10853-021-06608-4.

[5] P. Noorunnisa Khanam, M. A. Al Maadeed, M. Ouederni, E. Harkin-Jones, B. Mayoral, A. Hamilton, D. Sun, Melt processing and properties of linear low-density polyethylene-graphene nanoplatelet composites, *Vacuum*, 2016, **130**, 63-71, doi: 10.1016/j.vacuum.2016.04.022.

[6] H. J. Im, J. Y. Oh, S. Ryu, S. H. Hong, The design and fabrication of a multilayered graded GNP/Ni/PMMA nanocomposite for enhanced EMI shielding behavior, *RSC Advances*, 2019, **9**, 11289-11295, doi: 10.1039/c9ra00573k.

[7] H. J. Im, G. H. Jun, D. J. Lee, H. J. Ryu, S. H. Hong, Enhanced

electromagnetic interference shielding behavior of Graphene Nanoplatelet/Ni/Wax nanocomposites, *Journal of Materials Chemistry C*, 2017, **5**, 6471-6479, doi: 10.1039/c7tc01405h.
[8] P. Nimbalkar, A. Korde, R. K. Goyal, Electromagnetic interference shielding of polycarbonate/GNP nanocomposites in X-band, *Materials Chemistry and Physics*, 2018, **206**, 251-258, doi: 10.1016/j.matchemphys.2017.12.027.
[9] K. Sabira, M. P. Jayakrishnan, P. Saheeda, S. Jayalekshmi, On the absorption dominated EMI shielding effects in free standing and flexible films of poly(vinylidene fluoride)/graphene nanocomposite, *European Polymer Journal*, 2018, **99**, 437-444, doi: 10.1016/j.eurpolymj.2017.12.034.
[10] J. Joseph, A. K. Koroth, D. A. John, A. M. Sidpara, J. Paul, Highly filled multilayer thermoplastic/graphene conducting composite structures with high strength and thermal stability for electromagnetic interference shielding applications, *Journal of Applied Polymer Science*, 2019, **136**, 47792, doi: 10.1002/app.47792.
[11] P. Xie, Y. Liu, M. Feng, M. Niu, C. Liu, N. Wu, K. Sui, R. R. Patil, D. Pan, Z. Guo, R. Fan, hierarchically porous Co/C nanocomposites for ultralight high-performance microwave absorption, *Advanced Composites and Hybrid Materials*, 2021, **4**, 173-185, doi: 10.1007/s42114-020-00202-z.
[12] N. Wu, W. Du, Q. Hu, S. Vupputuri, Q. Jiang, Recent development in fabrication of Co nanostructures and their carbon nanocomposites for electromagnetic wave absorption, *Engineered Science*, 2021, **13**, 11-23, doi: 10.30919/es8d1149.
[13] B. Zhao, J. Deng, R. Zhang, L. Liang, B. Fan, Z. Bai, G. Shao, C. B. Park, Recent advances on the electromagnetic wave absorption properties of Ni based materials, *Engineered Science*, 2018, **3**, 5-40, doi: 10.30919/es8d735.
[14] S. Pratap, J. Khatri, P. Jain, D. Banga, Electromagnetic stress-a danger to human health, *International Journal of Emerging Technologies in Computational dan Applied Science*, 2014, **1**, 305-309.
[15] C. S. Cheung, Shielding effectiveness of superalloy, aluminum, and mumetal shielding tapes, Robert E. Kennedy Library, Cal Poly, 2009, doi: 10.15368/theses.2009.31.
[16] ASTM International, ASTM D638-10-Standard Test Method for Tensile Properties of Plastics, 2006, 1-15, doi: 10.1520/d0638-14.
[17] R. Shan, C. S. Yoo, J. H. Chen, T. Lu, Computational diagnostics for n-heptane flames with chemical explosive mode analysis, *Combustion and Flame*, 2012, **159**, 3119-3127, doi: 10.1016/j.combustflame.2012.05.012.
[18] E. A. Plis, D. P. Engelhart, J. Likar, R. C. Hoffmann, R. Cooper, D. Ferguson, Electrical behavior of carbon-loaded Kapton for spacecraft applications, *Journal of Spacecraft and Rockets*, 2018, **55**, 1-18, doi: 10.2514/1.A33970
[19] H. Gao, C. Wang, Z. Yang and Y. Zhang, 3D porous nickel metal foam/polyaniline heterostructure with excellent electromagnetic interference shielding capability and superior absorption based on pre-constructed macroscopic conductive framework, *Composites Science and Technology*, 2021, **213**, 108896, doi: 10.1016/j.compscitech.2021.108896.
[20] R. B. J. Chandra, B. Shivamurthy, S. Kulkarni, M. S. Kumar, Hybrid polymer composites for EMI shielding application- a review, *Materials Research Express*, 2019, **6**, 082008, doi: 10.1088/2053-1591/aaff00. 2019.
[21] R. K. Krishnaswamy, M. J. Lamborn, Tensile properties of linear low-density polyethylene (LLDPE) blown films, *Polymer Engineering & Science*, 2000, **40**, 2385-2396, doi: 10.1002/pen.11370.
[22] E. Hatfield, Multilayer Flexible Packaging: Second Edition, 2016, 147-152, doi: 10.1016/b978-0-323-37100-1.00011-9.
[23] M. Rahaman, D. Khastgir, A. K. Aldalbahi, Carbon-containing polymer composites. Singapore: Springer Singapore, 2019, doi: 10.1007/978-981-13-2688-2.
[24] K. Jagatheesan, A. Ramasamy, A. Das and A. Basu, Electromagnetic shielding behaviour of conductive filler composites and conductive fabrics-A review, *Indian Journal of Fibre and Textile Research*, 2014, **39**, 329-342.
[25] M. Peng and F. Qin, Clarification of basic concepts for electromagnetic interference shielding effectiveness, *Journal of Applied Physics*, 2021, **130**, 225108, doi: 10.1063/5.0075019.
[26] C. Wang, H. Gao, D. Liang, S. Liu, H. Zhang, H. Guan, Y. Wu, Y. Zhang, Effective fabrication of flexible nickel chains/acrylate composite pressure-sensitive adhesives with layered structure for tunable electromagnetic interference shielding, *Advanced Composites and Hybrid Materials*, 2022, 1-15, doi: 10.1007/s42114-022-00482-7.
[27] Y. Zhang, Z. Yang, T. Pan, H. Gao, H. Guan, J. Xu, Z. Zhang, Construction of natural fiber/polyaniline core-shell heterostructures with tunable and excellent electromagnetic shielding capability via a facile secondary doping strategy, *Composites Part A: Applied Science and Manufacturing*, 2020, **137**, 105994, doi: 10.1016/j.compositesa.2020.105994.
[28] Y. Zhang, M. Qiu, Y. Yu, B. Wen, L. Cheng, A novel polyaniline-coated bagasse fiber composite with core-shell heterostructure provides effective electromagnetic shielding performance, *ACS Applied Materials & Interfaces*, 2017, **9**, 809-818, doi: 10.1021/acsami.6b11989.
[29] Y. Zhang, Z. Yang, B. Wen, An ingenious strategy to construct helical structure with excellent electromagnetic shielding performance, *Advanced Materials Interfaces*, 2019, 1900375, doi: 10.1002/admi.201900375.

